

ELEVENTH EUROPEAN ROTORCRAFT FORUM

Paper No. 67

COMPARISON BETWEEN MEASURED AND CALCULATED STALL-FLUTTER BEHAVIOUR
OF A ONE-BLADED MODEL ROTOR

by

H. Bergh

A.J.P. van der Wekken

National Aerospace Laboratory NLR
The Netherlands

September 10-13, 1985
London, England.

THE CITY UNIVERSITY, LONDON, EC1V OHB, ENGLAND.

COMPARISON BETWEEN MEASURED AND CALCULATED STALL-FLUTTER BEHAVIOUR
OF A ONE-BLADED MODEL ROTOR

by

H. Bergh

A.J.P. van der Wekken

National Aerospace Laboratory NLR
The Netherlands

Abstract

In a low-speed windtunnel flutter tests are performed with a driven model rotor, consisting of one rigid blade hinged at the root by a weak bending-torsion spring. Many flutter points in non-stalled and stalled flow are measured with three different model configurations by changing the rotor speed at constant tunnel velocity.

Aerodynamic derivatives for the stall domain are deduced from the ONERA semi-empirical dynamic stall model for two-dimensional flow.

Application of these derivatives in flutter calculations for the model rotor shows a very good agreement with the experiments.

1 Introduction

It is almost 50 years ago that Studer (ref. 1) showed the existence of stall-flutter with his model experiments. Since then many investigations were devoted to this subject, but due to the complexity of the unsteady aerodynamics in the stall range the prediction of the phenomenon remained an illusion.

The development at ONERA of a semi-empirical calculation model for two-dimensional unsteady flow in the stall domain (refs. 2 and 3) encouraged the authors to apply this model into a stall-flutter investigation. The interest in this subject came from the Wind Energy Group at the Delft Technological University.

The present paper describes the flutter experiments with a one-bladed model rotor, the deduction of unsteady aerodynamic derivatives from the ONERA modelling and their application to flutter calculations for the model rotor.

2 The flutter experiments

2.1 Test set-up and test procedure

The model used consists of one rigid blade of constant chord fixed to a relatively weak spring strip at the root (fig. 1). The blade section is NACA 0012 and the elastic axis coincides with the quarter chord axis. At the root chord a special yoke with variable masses is fixed to the rotorblade (fig. 2) in order to change frequencies and mass coupling. The blade has a linear twist of 5.7° between root and tip.

The model rotor is driven by an electric motor. During the flutter tests, the rotor was placed in the open jet low-speed windtunnel (diameter 2.20m) of the Aerospace Department of the Delft Technological University. The tip chord was almost in the plane of rotation, and due to the twist, the rootchord had about 6 degrees incidence (with the leading edge more upstream). The tunnel flow was perpendicular to the plane of rotation.

The damping of the model at rest is very low. Expressed as a hysteresis damping, the measured damping values for flapping and torsion are $h_\beta = 0.001$ and $h_\theta = 0.0025$ respectively.

For the flutter test the following test procedure was chosen. First the tunnelspeed was set to the desired value and then the rotational speed of the rotor was raised gradually until the amplitude of torsion started to grow. The latter was indicated on an oscilloscope by the signal of a strain gauge bridge at the spring strip. In this way three different model configurations, obtained by the mass positions indicated in fig. 3, were tested.

2.2 Results of the flutter tests

Two series of flutter tests were conducted. First, all three configurations were tested with natural boundary layer transition. However, for such low Reynolds numbers large boundary layer effects on oscillating wings were observed earlier by the first author (ref. 4). Therefore the tests with the configurations 1 and 3 were repeated with a trip wire at both model surfaces. The trip wire used was 0.15 mm thick and 3 mm wide and located between 7 and 10 percent of the chord.

The results for configurations are shown in fig. 4 in dependence of the tunnel speed V and the rotor speed Ω . The ratio between these two parameters determines the local angle of attack. To facilitate the discussion a few straight lines for constant angle of attack at a reference section at $0.75R$ are indicated.

At small angles of attack upto at least $\alpha_{ref} = 7^\circ$ the classical flapping-torsion flutter with attached flow occurs. At higher angles of attack the effect of local stall leads to a drastic decrease in flutter speed. However, at slightly higher values of α_{ref} the flutter speed is raised suddenly in spite of the detached flow. The latter phenomenon shows a marked influence of the trip wire. Without trip wire restabilization occurs at $\alpha_{ref} \approx 12.1^\circ$, while with trip wire this effect is delayed till $\alpha_{ref} \approx 14.4^\circ$.

For configuration 2 only results without trip wire are available. The results in fig. 5 show the same tendency with angle of attack as for configuration 1. Even restabilization occurs at almost the same α_{ref} .

In fig. 6 the results for configuration 3 are presented. This picture is a degenerated version of the previous figures. Again at low angles of attack flapping-torsion flutter is observed. Stall-flutter is limited to a very narrow range of angles of attack. The trip wire again has a distinct influence on stall-flutter. It is remarkable that with and without trip wire the restabilization occurs at the same α_{ref} as for configuration 1.

Stroboscopic observations revealed that during stall-flutter in all three cases the rotorblade oscillated mainly in torsion.

3 The calculation method for the aerodynamic forces

3.1 The ONERA semi-empirical model

The calculation method is based on the semi-empirical model for two-dimensional flow developed at ONERA during the last years (refs. 2 and 3). For attached flow lift and moment are linear and deduced from the following two equations.

$$\dot{F} + \lambda F = \frac{1}{2} \rho V^2 c \left\{ \lambda c_{\ell \alpha} (\theta + \dot{h}) + \lambda s \theta + \sigma (\dot{\theta} + \ddot{h}) + s \ddot{\theta} \right\} \quad (1)$$

$$M = \frac{1}{2} \rho V^2 c^2 \left\{ c_{m \alpha} (\theta + \dot{h}) + s_m \dot{\theta} + \sigma_m (\dot{\theta} + \ddot{h}) + s_m \ddot{\theta} \right\} \quad (2)$$

with h and θ being the (dimensionless) amplitudes of translation and rotation while a $(\dot{})$ means differentiation to the dimensionless time $\tau = 2Vt/c$. The coefficients λ , s , σ , s_m and σ_m are given in detail in ref. 3 as function of Mach number.

In the stall domain, for lift as well as for moment the following extra equation is added that gives a correction to the linear lift and moment:

$$\ddot{F}_c + a \dot{F}_c + r F_c = -\frac{1}{2} \rho V^2 c \left\{ r \Delta c_{\ell} + E (\dot{\theta} + \ddot{h}) \right\} \quad (3)$$

$$\ddot{M}_c + a_m \dot{M}_c + 2 M_c = -\frac{1}{2} \rho V^2 c^2 \left\{ r_m \Delta c_m + E_m (\dot{\theta} + \ddot{h}) \right\} \quad (4)$$

Again the coefficients are presented in ref. 3 as function of Mach number and the main stall parameter Δc_{ℓ} , being the dimensionless lift loss with respect to the extrapolated linear value.

So in the stall domain, the total lift and total moment are

$$F_{tot} = F + F_c$$

$$M_{tot} = M + M_c$$

Application of the ONERA equations in a flutter calculation leads to extensive calculations of the response versus time, e.g. by numerical integration of the equations of motion.

3.2 The small oscillation method

The aerodynamic derivatives for two-dimensional attached flow, defined by, e.g.

$$F = \pi\rho V^2 c/2(k_a h + k_b \theta) \quad (5)$$

$$M = \pi\rho V^2 c^2/4(m_a h + m_b \theta) \quad (6)$$

can be expressed in terms of the coefficients of eqs. (1) and (2). Substituting equations (5) and (6) into the left hand side of equations (1) and (2), yields the following relations:

$$\begin{aligned} k'_a &= \lambda k^2 \frac{c_{l_\alpha} - \sigma}{k^2 + \lambda^2} & k''_a/k &= c_{l_\alpha} - \frac{k'}{\lambda} \\ k'_b &= c_{l_\alpha} - \frac{k'}{\lambda} & k''_b/k &= s - \lambda \frac{c_{l_\alpha} - \sigma}{k^2 + \lambda^2} \\ m'_a &= -k^2 \sigma_m & m''_a/k &= c_{m_\alpha} \\ m'_b &= c_{m_\alpha} - k^2 s_m & m''_b/k &= s_m + \sigma_m \end{aligned}$$

In the stall domain lift and moment vary strongly non-linear with the angle of attack. However small harmonic oscillations around a certain angle of attack in that range still generate harmonic variations of lift and moment, as is demonstrated in fig. 7. That means that for a chosen mean angle the flutter problem may be solved with (local) linearized aerodynamics resulting at least in a stability boundary for small oscillations.

To derive the aerodynamic derivatives for stall-flutter calculations from the ONERA data, a similar approach is followed as for the linear case. This will be described in detail in ref. 5.

For the oscillatory parts the following expressions are introduced, that give corrections to the linear values:

$$F_c = -\pi\rho V^2 c/2(k_{a_c} h + k_{b_c} \theta) \quad (7)$$

$$M_c = -\pi\rho V^2 c^2/4(m_{a_c} h + m_{b_c} \theta) \quad (8)$$

Substituting these relations into the left hand side of eqs. (3) and (4) and equating the corresponding terms, yields:

$$k'_{a_c} = k^2 \frac{-E(r-k^2) + ar\Delta c_{l_\alpha}}{a^2 k^2 + (r-k^2)^2}$$

$$k''_{a_c} / k = \frac{aEk^2 + r\Delta c_{l_\alpha}(r-k^2)}{a^2 k^2 + (r-k^2)^2}$$

$$k'_{b_c} = \frac{r\Delta c_{l_\alpha}(r-k^2) + aEk^2}{a^2 k^2 + (r-k^2)^2}$$

$$k''_{b_c} / k = -\frac{ar\Delta c_{l_\alpha} - E(r-k^2)}{a^2 k^2 + (r-k^2)^2}$$

$$m'_{a_c} = k^2 \frac{E_m(r_m-k^2) - a_m r_m \Delta c_{m_\alpha}}{a_m^2 k^2 + (r_m-k^2)^2}$$

$$m''_{a_c} / k = -\frac{a_m E_m k^2 + r_m \Delta c_{m_\alpha} (r_m-k^2)}{a_m^2 k^2 + (r_m-k^2)^2}$$

$$m'_{b_c} = \frac{-r_m \Delta c_{m_\alpha} (r_m-k^2) - a_m E_m k^2}{a_m^2 k^2 + (r_m-k^2)^2}$$

$$m''_{b_c} / k = \frac{a_m r_m \Delta c_{m_\alpha} - E_m (r_m-k^2)}{a_m^2 k^2 + (r_m-k^2)^2}$$

with $\Delta c_{l_\alpha}(\alpha_0) = c_{l_\alpha} - c_{l_\alpha}(\alpha_0)$
 $\Delta c_{l_\alpha}(\alpha_0) = c_{l_\alpha} - c_{l_\alpha}(\alpha_0)$

$\Delta c_{m_\alpha}(\alpha_0) = c_{m_\alpha} - c_{m_\alpha}(\alpha_0)$
 $\Delta c_{m_\alpha}(\alpha_0) = c_{m_\alpha} - c_{m_\alpha}(\alpha_0)$

A great advantage of the aerodynamic derivatives for the stall-domain is that the ONERA data are applicable directly into existing flutter programs.

4 Calculated results and discussion

4.1 The scope of the calculations

The coefficients in the expressions for the aerodynamic derivatives are taken from appendices VI-4 and VI-5 of ref. 3, which are meant to be valid for a general model. As differences exist in sign, in dimensionalizing and between the use of radians or degrees, values consistent with the notation of ref. 7 are given in the appendix.

To account as well as possible for the low Reynolds numbers in the tests, the lift and moment curves for NACA0012 are taken from ref. 6 for $Re = 0.36 \times 10^6$. The approximations used with their derivatives are presented too in the appendix. Furthermore the figs. 8 and 9 show the measured c_{l_α} -a curve and c_{m_α} -a curve with the approximation used.

In the flutter calculations two degrees of freedom are used, linear bending (flapping) and a constant torsion of the rotorblade. The effect of the radial position on the aerodynamics is taken into account in a rather simple way. The rotorblade is divided into three equal parts and for each part the aerodynamic derivatives at the mid section are used. Furthermore, some calculations are made with aerodynamic derivatives equal to those of one reference section at .75R.

4.2 Results and discussion

In fig. 10 the calculated results are presented in comparison with the measured flutter points. In the stall domain the agreement between the more sophisticated calculations and the experiments with trip wire is remarkably well. The discrepancies for the flapping-torsion flutter at low angles of attack stem from the ONERA approximation for the linear derivatives. The latter is clear from the flutter speed calculated with the usual instationary aerodynamics of ref. 7. Fig. 10 also demonstrates, that the old "trick" of taking a reference section at 75 percent gives good results.

The calculations for configuration 2 (fig. 11) show more discrepancies with experiment. However, it is plausible from section 2.2 that with a trip wire restabilization should be delayed by about 2.2° leading to an improved correlation.

The hard case of configuration 3 (fig. 12) reveals a striking correspondance between the measurements with trip wire and the more extensive calculations. However, even the simple flutter calculation may be used in this case as a prediction method for stall-flutter.

An appreciable improvement is obtained for configuration 1 when the approximations for the linear aerodynamic derivatives are replaced by the theoretical values of ref. 7. As shown in fig. 13 not only the classical flutter prediction is improved, but also the discrepancies in the stall-flutter domain disappear for the greater part. Similar calculations for configuration 3 (fig. 14) lead to identical conclusions for the classical flutter. The stall-flutter results however, are hardly affected by the introduction of theoretical, linear derivatives. So it may be concluded that for angles of attack from zero to far beyond the stall angle, linear theory combined with the aerodynamic derivatives for the stall domain (pt. 3.2) may be used successfully in flutter-calculations.

Studer in his early experiments (ref. 1) already demonstrated stall-flutter with one degree of freedom (torsion only). The question arises now, whether a calculation with only torsional oscillations might predict the present stall-flutter results sufficiently. In fig. 15 the stall-flutter boundaries for one and two degrees of freedom are presented. The predominant influence of torsion is obvious, but yet flapping is needed for a better agreement with the experiments. This is not always the case as appears from similar calculations for configuration 3 shown in fig. 16.

Apparently configuration 3 performs mainly torsional oscillations. This explains why in this case the introduction of linear theoretical derivatives hardly affects the stall-flutter results (see fig. 14). In flutter with pure torsion, only the derivative m_b plays a part and for incompressible flow the ONERA-approximation for the linear value of m_b is exact.

5 Concluding remarks

The usefulness of the proposed aerodynamic derivatives for the stall domain is demonstrated by the agreement between the flutter calculations and so many measured flutter points. As the aerodynamics used is deduced from the ONERA semi-empirical stall model, the present results clearly emphasize the fitness of that model.

Although the present investigation is restricted to incompressible flow, the aerodynamic derivatives for the stall-domain have a wider application. The effect of compressibility can be taken into account easily as Mach number is already included in the related ONERA-expressions. Furthermore the application is not restricted to rotorblades. Flutter problems of fixed wings with planforms that allow a meaningful use of aerodynamic derivatives for two-dimensional flow may be handled too.

Finally, expressing the effect of stall into a few aerodynamic derivatives has the advantage that existing simple computerprograms for flutter can be used. However, it must be realized that the derivatives are only valid for small oscillations, which restricts their use mainly to flutter problems.

Acknowledgement: The authors wish to express their thanks to Mr. K.P. Jessurun of the Aerospace Department at Delft, who designed such a magnificent model rotor and who had an active part in the windtunnel experiments.

6 References

- 1) H.L. Studer. Experimentele Untersuchungen über Flügelschwingungen, Mitt. Inst. Aerodynamik ETH Zürich Nr. 4/5, 1936
- 2) C.T. Tran, D. Petot. Semi-empirical model for the dynamic stall of airfoils in view of the application to the calculation of responses of a helicopter blade in forward flight, Paper presented at 6th European Rotorcraft Forum, Bristol, 1980
- 3) D. Petot. Progress in the semi-empirical prediction of the aerodynamic forces due to large amplitude oscillations of an airfoil in attached or separated flow. Paper presented at 9th European Rotorcraft Forum, Stresa, 1983
- 4) J.H. Greidanus, A.J. van de Vooren, H. Bergh. Experimental Determination of the aerodynamic characteristics of an oscillating wing with fixed axis of rotation. NLL Report F101, 1952
- 5) H. Bergh. Aerodynamic derivatives for stall-flutter calculations. To be published by NLR.
- 6) R.E. Sheldahl, P.C. Klimas. Aerodynamic characteristics of seven symmetrical airfoil sections through 180-degree angle of attack for use in aerodynamic analysis of vertical axis wind turbines. Sandia Nat. Lab. Report SAND 80-2114, 1981
- 7) A.J. van de Vooren. Collected tables and graphs of theoretical two-dimensional linearized aerodynamic coefficients for oscillating wings. NLR Report F235, 1963.

Appendix

The following expressions are obtained from ref. 3 and used in the formulae of section 3.2.

Linear domain

$$\lambda = 0.25 - 0.15M^2$$

$$s = \frac{180}{\pi^2} \left\{ 0.08(1 + M^2) \right\}$$

$$\sigma = b - \lambda s \text{ with } b = \frac{180}{2} (0.105 + 0.1\Delta c_{\ell} - 0.08M)$$

$$s_m = -0.47 - \frac{1.8}{\pi} \arctan 15(M-0.7)$$

$$\sigma_m = b_m - s_m \text{ with } b_m = 1 + 1.4M^2$$

For $M = 0$

$$\lambda = 0.25$$

$$s = 1.46 \quad s_m = 0.375$$

$$\sigma = 1.55 \quad \sigma_m = 0.625$$

Stall-domain

$$\sqrt{r} = \sqrt{r_m} = -0.9 + 0.65\Delta c_{\ell} + \frac{1}{1 + 0.65\Delta c_{\ell}}$$

$$a = a_m = 0.15 + 0.45\Delta c_{\ell}^2$$

$$E = \frac{180}{2} (-0.08\Delta c_{\ell}^2)$$

$$E_m = \frac{360}{\pi^2} (+0.02\Delta c_{\ell}^2)$$

For the static values the approximations are:

Lift:

$$0 \leq \alpha < 10 \quad c_{\ell} = 0.12 \alpha - 0.0003 \alpha^3$$

$$10 \leq \alpha \leq 20 \quad c_{\ell} = 2.05 - 0.152 \alpha + 0.0033 \alpha^2 + 0.00004 \alpha^3$$

$$20 < \alpha \leq 26 \quad c_{\ell} = 0.025 \alpha$$

Moment:

$$0 \leq \alpha < 9 \quad c_m = 0.0001097 \alpha^3 - 0.00000914 \alpha^4$$

$$9 \leq \alpha \leq 15 \quad c_m = -1.3298 + 0.375 \alpha + 0.33336 \alpha^2 + 0.000926 \alpha^3$$

$$\alpha > 15 \quad c_m = -0.08$$

For use in the expressions of section 3.2 the following derivatives are deduced from these approximations

$$\Delta c_{\ell} = 0.12 \alpha - c_{\ell}$$

$$\Delta c_{\ell \alpha} = \frac{180}{\pi^2} \left(0.12 - \frac{\partial c_{\ell}}{\partial \alpha} \right)$$

$$\Delta c_{m \alpha} = \frac{360}{\pi^2} \left(0 - \frac{\partial c_m}{\partial \alpha} \right)$$

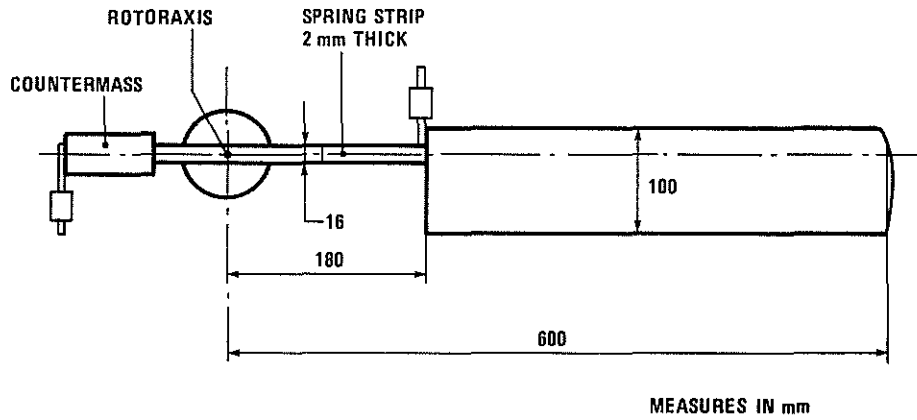


Fig. 1 Model dimensions

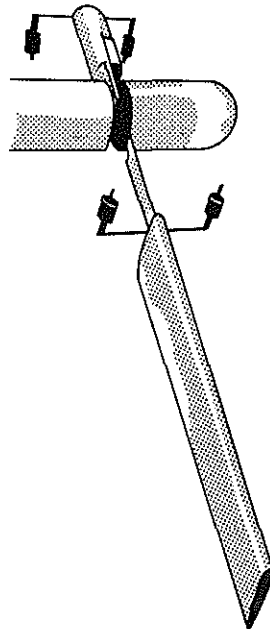


Fig. 2 Model with yoke

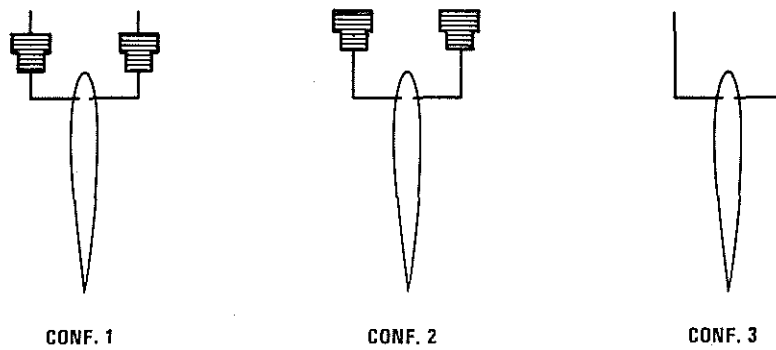


Fig. 3 Mass locations for the 3 configurations

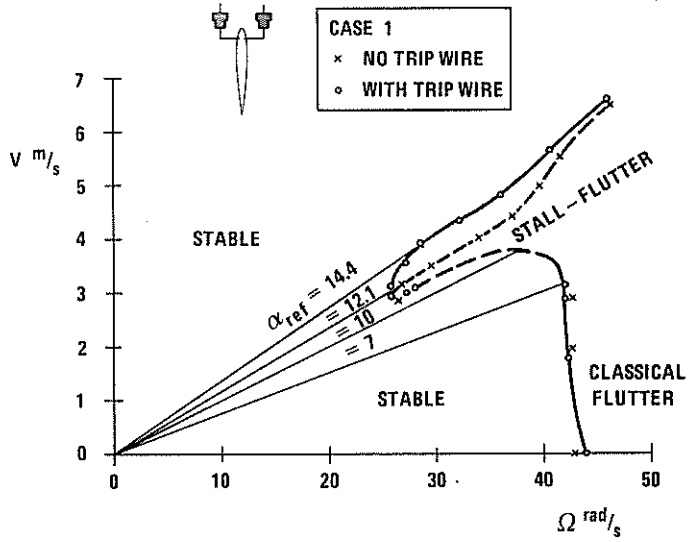


Fig. 4 Experimental results for configuration 1

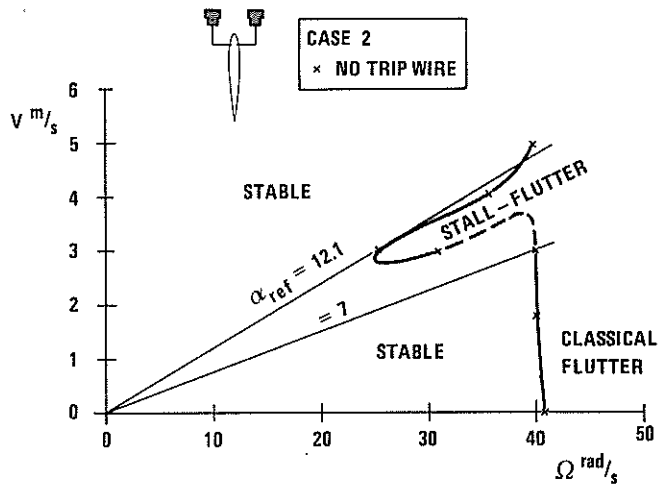


Fig. 5 Experimental results for configuration 2

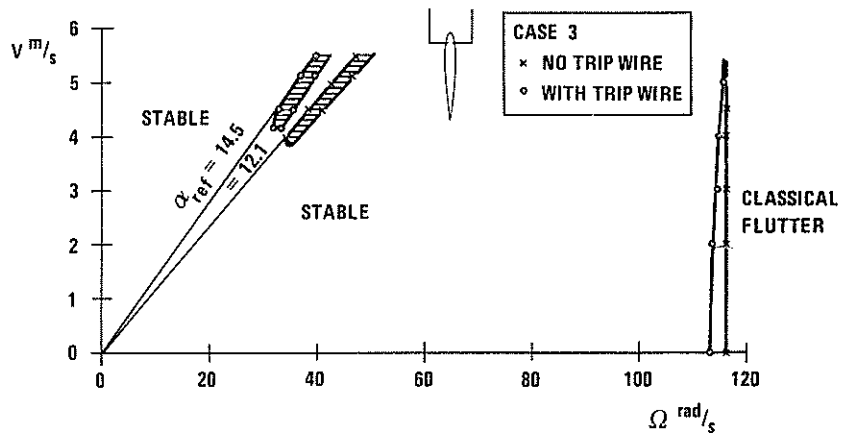


Fig. 6 Experimental results for configuration 3

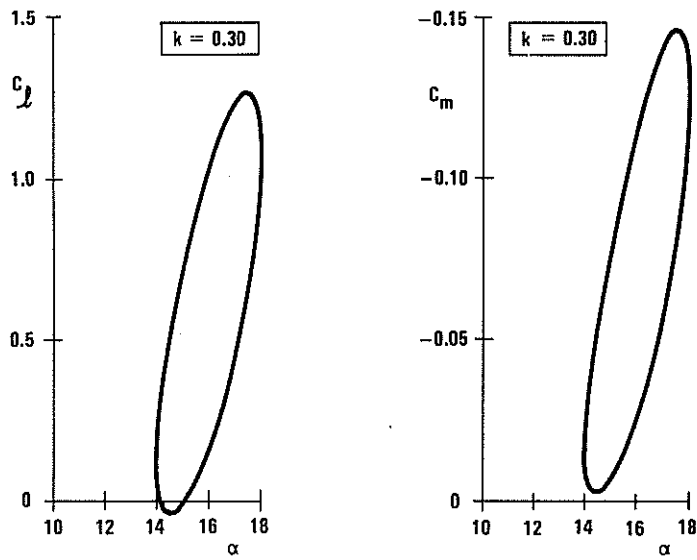


Fig. 7 Lift and moment, due to an harmonic rotation

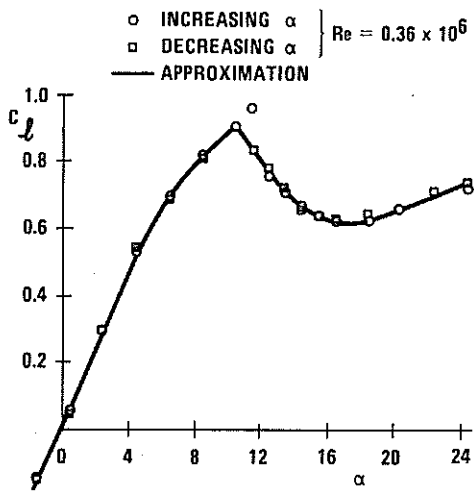


Fig. 8 Approximated c_l - α curve

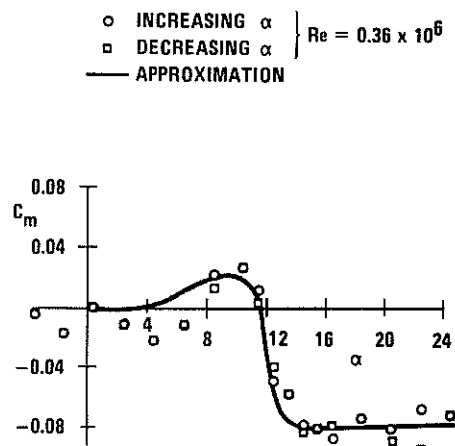


Fig. 9 Approximated c_m - α curve

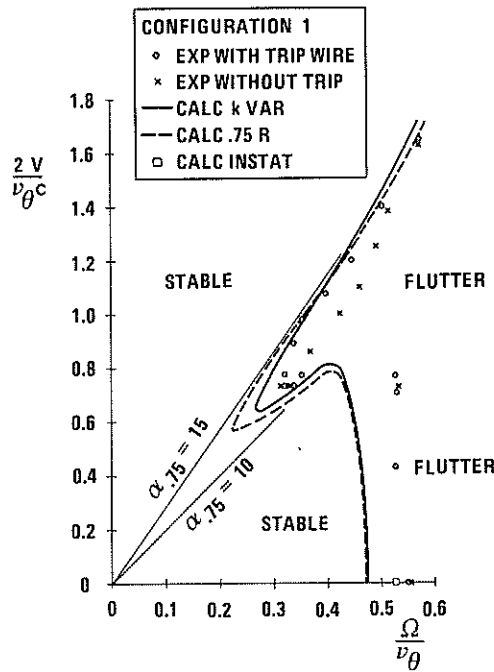


Fig. 10 Calculated results for configuration 1

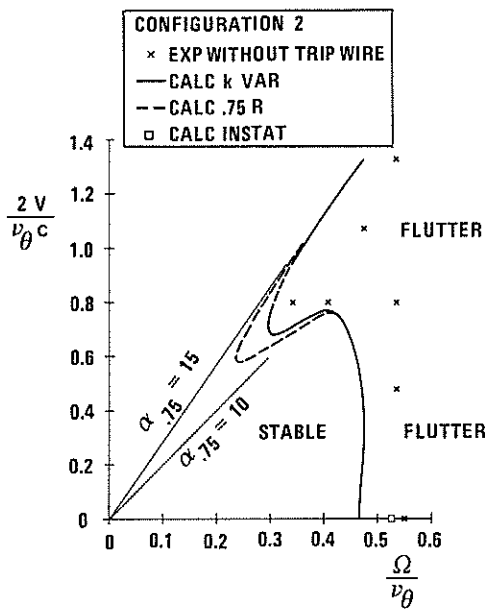


Fig. 11 Calculated results for configuration 2

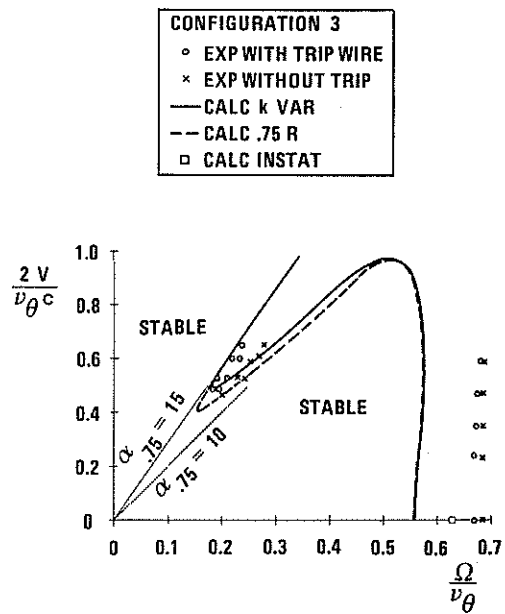


Fig. 12 Calculated results for configuration 3

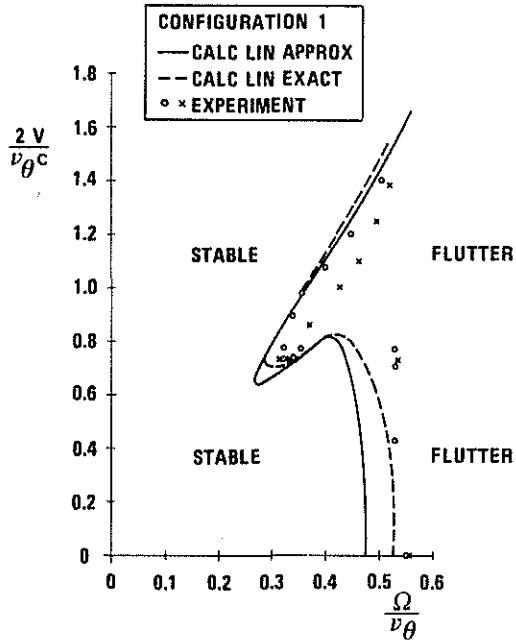


Fig. 13 Calculation with theoretical linear derivatives

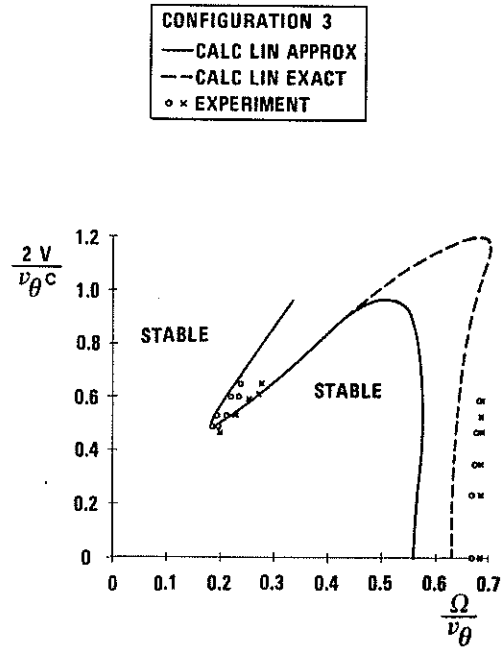


Fig. 14 Calculation with theoretical linear derivatives

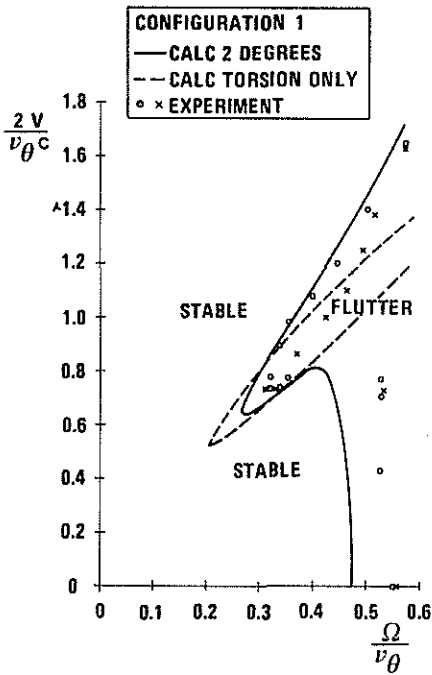


Fig. 15 Calculation with one and two degrees of freedom

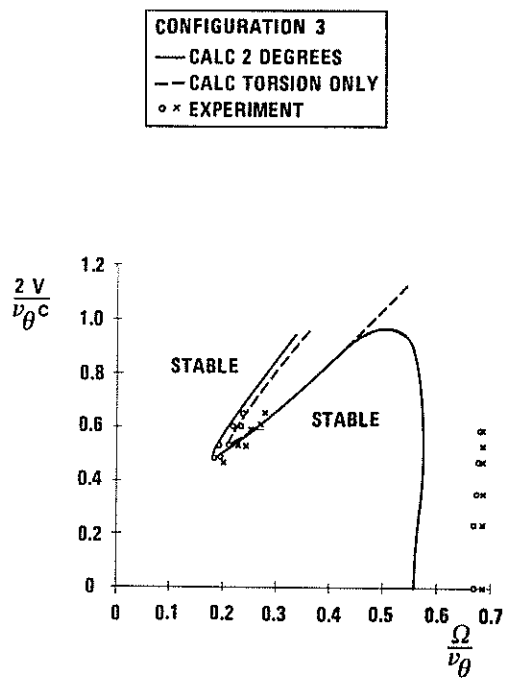


Fig. 16 Calculation with one and two degrees of freedom